Tough and tunable adhesion of hydrogels: experiments and models

Citation: Zhang, Teng; Yuk, Hyunwoo et al. "Tough and Tunable Adhesion of Hydrogels: Experiments and Models." Acta Mechanica Sinica 33, 3 (May 2017): 543–554 © 2017 The Chinese Society of Theoretical and Applied Mechanics; Institute of Mechanics, Chinese Academy of Sciences and Springer-Verlag Berlin Heidelberg

As Published: http://dx.doi.org/10.1007/s10409-017-0661-z

Publisher: Springer-Verlag

Persistent URL: http://hdl.handle.net/1721.1/110619

Version: Author's final manuscript: final author's manuscript post peer review, without publisher's formatting or copy editing

The DOI for this manuscript is doi: .

Please use the following full citation:

Zhang, T., Yuk, H., Lin, S., Parada, G. A., Zhao, X.: Tough and Tunable Adhesion of Hydrogels: Experiments and Models. Acta Mechanica Sinica., doi: , in press.

Tough and Tunable Adhesion of Hydrogels: Experiments and Models

Teng Zhang[1,2a], Hyunwoo Yuk[2a], Shaoting Lin[2], German A. Parada[2], Xuanhe Zhao[2,3*]

[1.] Department of Mechanical and Aerospace Engineering, Syracuse University, Syracuse, NY 13244, USA; [2.] Soft Active Materials Laboratory, Department of Mechanical Engineering, Massachusetts Institute of Technology, Cambridge, MA 02139, USA; [3.] Department of Civil and Environmental Engineering, Massachusetts Institute of Technology, Cambridge, MA 02139, USA

[a.] These authors contribute equally to the current work

* Corresponding author. Email: zhaox@mit.edu

Abstract

As polymer networks infiltrated with water, hydrogels are major constituents of animal and plant bodies and have diverse engineering applications. While natural hydrogels can robustly adhere with other biological materials such as bonding of tendons and cartilages on bones and adhesive plaques of mussels, it is challenging to achieve such tough adhesions between synthetic hydrogels and engineering materials. Recent experiments show that chemically anchoring long-chain polymer networks of tough synthetic hydrogels on solid surfaces can give adhesions tougher than their natural counterparts, but the underlying mechanism has not been well understood. It is also challenging to systematically tune the adhesion of hydrogels on solids. Here, we provide a quantitative understanding of the mechanism for tough adhesions of hydrogels on solid materials via a combination of experiments, theory and numerical simulations. Using a coupled cohesive-zone and Mullins-effect model validated by experiments, we reveal the interplays of intrinsic work of adhesion, interfacial strength and energy dissipation in bulk hydrogels in order to achieve tough adhesions. We further show that hydrogel adhesion can be systematically tuned by tailoring the hydrogel geometry and silanization time of solid substrates, corresponding to the control of energy dissipation zone and intrinsic work of adhesion, respectively. The current work further provides a theoretical foundation for rational design of future biocompatible and underwater adhesives.

Keywords Adhesion, Hydrogels, Soft materials, Mullins effect

1. Introduction

As polymer networks infiltrated with water, hydrogels are major constituents of animal bodies. While the soft and wet nature of hydrogels enables flexibility and transport of biomolecules, it also makes hydrogels by themselves unsuitable to serve as stiff load-bearing structures. Therefore, hybrid structures of hard materials such as bones and soft hydrogels such as tendons and cartilages are widely found in nature. Robust adhesions of the hydrogels on the diverse solids are critical to maintain the integrations of these biological hybrid structures. For example, in many animals the interfacial toughness of cartilages on bones and tendons on bones can reach up to 800 J/m^2 [1, 2]. Tough bonding of hydrogels can also be found in mussel plaques adhered on rocks [3-5], which is crucial for the survival of mussels under harsh environments with repeated wave impacts.

Hydrogels also have important technological applications in areas as diverse as tissue engineering and drug delivery [6, 7], biocompatible stretchable electronics [8, 9], actuators for optics [10] and microfluidics [11], soft robotics and machines [12]. In many applications, it is critical to achieve robust adhesions between hydrogels and solid materials such as metal, ceramic, silicon and polymers in order to maintain robust integrations and proper functions of hydrogels in the devices and systems. However, it has been challenging to robustly bond synthetic hydrogels on engineering solids [13] and the interfacial toughness between synthetic hydrogels and solids is usually much lower than their natural counterparts [14]. For example, nanocomposite hydrogels with crosslinked poly(ethylene glycol) and silicate were found to adhere to various surfaces [15] with interfacial toughness at the level of 10 to 30 J/m^2. Rose et al. [16] recently developed a nanoparticle-based glue for hydrogels and biological tissues and demonstrated the capability of wet adhesion with interfacial toughness from 1.6 to 25 J/m^2.

Studying the robust adhesion of mussel plaques, it was found that amino acid 3,4-dihydroxy-L-phenylalanine (DOPA) plays a crucial role in the underwater adhesion [17-20]. A great number of DOPA based adhesive hydrogels have been developed and found to have moderate adhesion (interfacial toughness less than 100 J/m^2) [21-24]. For a special case of porous solid substrate, Kurokawa et al. [25] reported a strong interface due to locking deformation of the double network hydrogel inside the solid pores. However, the adhesion performances of the synthetic hydrogels on common (nonporous) solid surfaces are still far below their biological counterparts such as cartilages on bones and mussel's plaques on rocks.

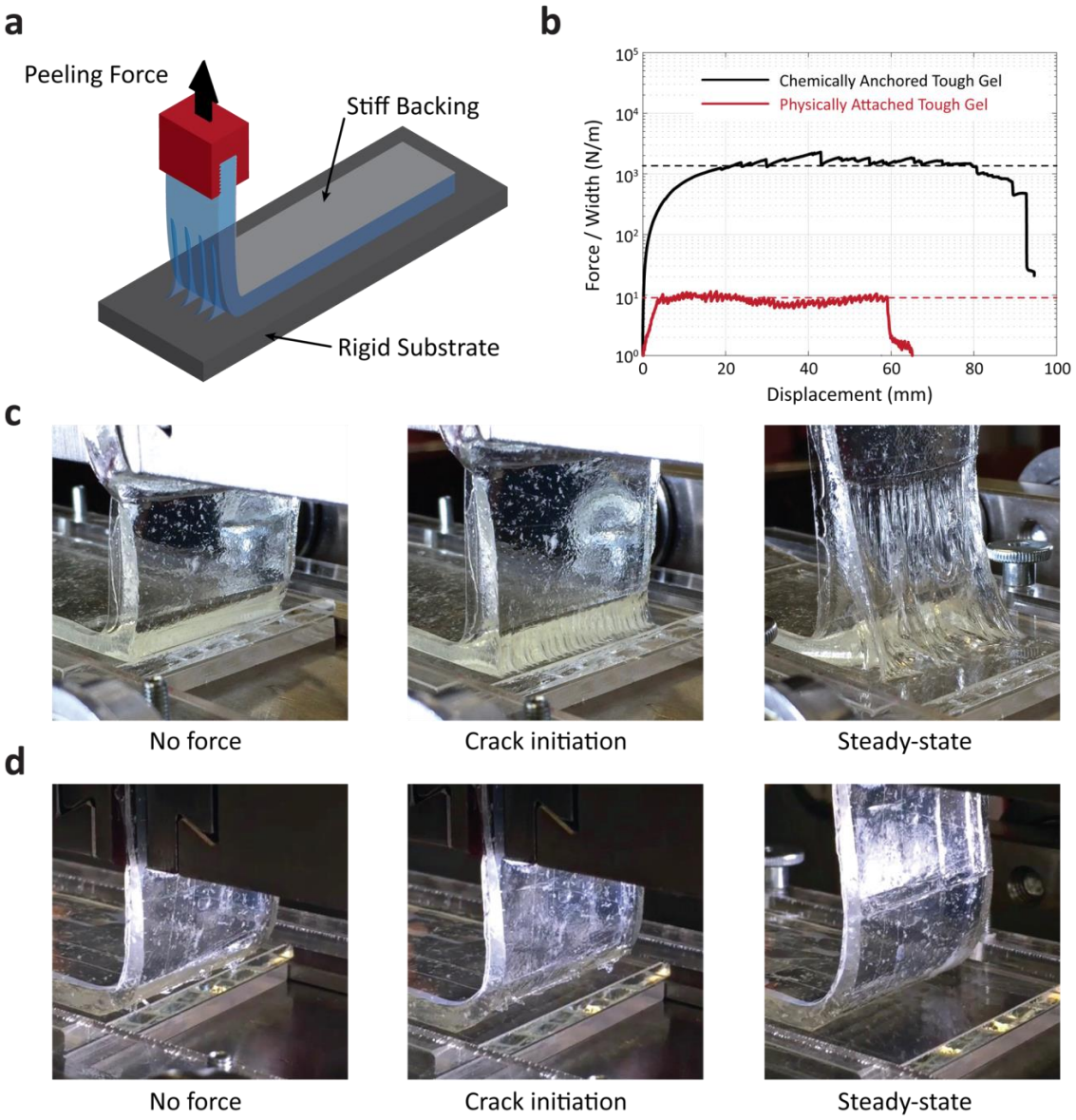

Fig. 1 a Schematic show of the peeling test. **b** Curves of the peeling force per width of hydrogel sheet versus displacement for hydrogels with and without chemically anchors on the solid surface. **c** Photos of the peeling process of a tough hydrogel with its long-chain network chemically anchored on a glass substrate. **d** Photos of the peeling process of a tough hydrogel physically attached on a glass substrate.

A breakthrough in the field was recently made by Yuk et al. [26, 27], who developed a strategy to achieve tough bonding of hydrogels on various nonporous solids via chemically anchoring the stretchy polymer networks of tough hydrogels to the solid surfaces. Through peeling tests (Fig. 1a), the interfacial toughness of the bonding was measured to be over 1,500 J/m^2 (Fig. 1b). Furthermore, only minor reductions of the interfacial toughness were found after swelling the hydrogel-solid structures in water, showing high robustness of the bonding in wet environments. It was experimentally demonstrated that the chemical anchorages of stretchy polymer networks of tough hydrogels on solid surfaces and energy dissipation of bulk hydrogels (see Fig. 1b-c) were the key factors to achieve tough bonding of hydrogels on solids [27]. Consistently, very weak adhesion was found for tough hydrogels only physically attached to solid substrates without chemical bonds (Fig. 1d). This design strategy is expected to enhance the interfacial toughness of various hydrogel-solid hybrids for diverse applications and thus calls for more in-depth theoretical understanding of the mechanisms of the tough bonding. Furthermore, such fundamental understanding can also shed light on the mechanisms for tough adhesions of biological hydrogels such as mussel's plaques [4].

While the toughening mechanisms of hydrogel adhesion have been rarely studied, there has been significant research on adhesion of elastomers, which is relevant to hydrogel adhesions and thus briefly reviewed as follow. It is known that the adhesion between two materials is not only determined by the interfacial properties, such as interfacial strength and intrinsic work of adhesion, but also by the bulk properties of the materials, such as viscoelasticity, plasticity and fracture toughness [28-31]. Ahagon and Gent [32] investigated the adhesion of an elastomer layer on a rigid substrate with various types of interfacial chemical bonds and found the chemical bonds can dramatically influence the interfacial toughness. Most soft elastomeric adhesives

exhibit strong rate-dependent adhesion behaviors [33-35], which are largely attributed to the viscoelasticity of the elastomers [36-38]. The plasticity of bulk materials was also found to have a significant effect on adhesion [39-41], especially for the adhesion of elastomers on metals [40]. If a relatively brittle material is bonded with a tough interface, the failure mode can switch from the interfacial failure to the cohesive failure of the bulk materials [34, 40], therefore the fracture toughness of the bulk materials can become the limit of the interfacial toughness. Surface roughness has also been found to play an important role in elastomer adhesion [25, 42, 43]. For example, Hoefnagels et al. [43] showed that the work of separation of a rough copper-rubber interface can reach over 1,000 J/m^2, which was attributed to the energy dissipation stored in the formation, deformation and rupture of fibrils between elastomers and the extra rough surfaces [44-46].

Previous studies on elastomer adhesions have been focused on the effects of viscoelasticity, plasticity and fracture toughness of the elastomers. Since significant energy dissipations in hydrogels, usually manifested as Mullins effect, have only been achieved recently [47, 48], few studies have been conducted to understand the role of Mullins effects on hydrogel adhesions. Our group recently showed that the Mullins effect is one key factor for hydrogels to achieve high fracture toughness [49]. It is expected that the energy dissipation from Mullins effect inside a process zone near the interfacial crack will contribute to the interfacial toughness [26, 27]. However, a quantitative understanding on the interactions between intrinsic work of adhesion and Mullins effect is still missing in studies of hydrogel adhesions.

Here we systemically examine the fundamental mechanisms underlying the tough adhesions of hydrogels on various solid surfaces. The rest of the paper is organized as follows. Section 2 presents the experimental measurements on the interfacial toughness of hydrogels on

solid substrates. Section 3 discusses the coupled Mullins-effect and cohesive-zone model for the simulations of peeling tests. Validation of the model and comparisons between simulation results and experimental data are shown in Sect. 4. Section 5 explores the design principles for tough and tunable adhesion of hydrogels by varying materials parameters, including interfacial strength and maximum energy dissipation. Concluding remarks and outlook are given in Sect. 6.

2. Experiments

The interfacial toughness of hydrogels bonded on glass substrates is measured using the standard 90° peeling test (ASTM D 2861) with mechanical testing machine (2 kN load cell; Zwick / Roell Z2.5) and 90° peeling fixture (G50; Test Resources). Borosilicate glass substrates are prepared with 7.62 cm in width, 12.7 cm in length and 0.32 cm in thickness. Before bonding hydrogels, the substrates are treated with silane solution following the previously reported method [27] to covalently bond stretchy polymer networks of the hydrogels on the substrate surfaces. Hydrogels are prepared and bonded on the substrates by curing hydrogel pre-gel solution within acrylic mold with area of 110 mm × 30 mm. The thickness of hydrogels is controlled by using glass spacers with different heights (0.1-6 mm). As a stiff backing for the hydrogel, silane-treated ultrathin glass films are used with an additional protective layer of transparent Scotch tape (3M) on top of the glass film (with thickness of 25 μm). The prepared samples are tested with the standard 90° peeling test setup (Fig. 1a). All the peeling tests are carried out with the constant peeling speed of 50 mm/min, which is slow enough to neglect the contribution from bulk viscosity of hydrogels [27]. The measured force reaches a plateau as the peeling process enters steady state, and this plateau force is calculated by averaging the measured force values in the steady-state region with common data processing software (Fig. 1b).

The interfacial toughness Γ is determined by dividing the plateau force F by the width of the hydrogel sheet W. In all experiments, polyacrylamide-alginate tough hydrogels with the physical and chemical hybrid crosslinks are used. Briefly, the polyacrylamide-alginate tough hydrogels are synthesized by mixing 10 mL of a carefully degassed aqueous pre-gel solution (12.05 wt.% acrylamide, 1.95 wt.% sodium alginate, 0.017 wt.% β-methylamino L-alanine (MBAA) and 0.043 wt.% ammonium persulfate) with calcium sulfate slurry (0.1328 times the weight of sodium alginate) and tetramethylethylenediamine (TEMED) (0.0025 times the weight of acrylamide) following the previous reported protocols [27, 48].

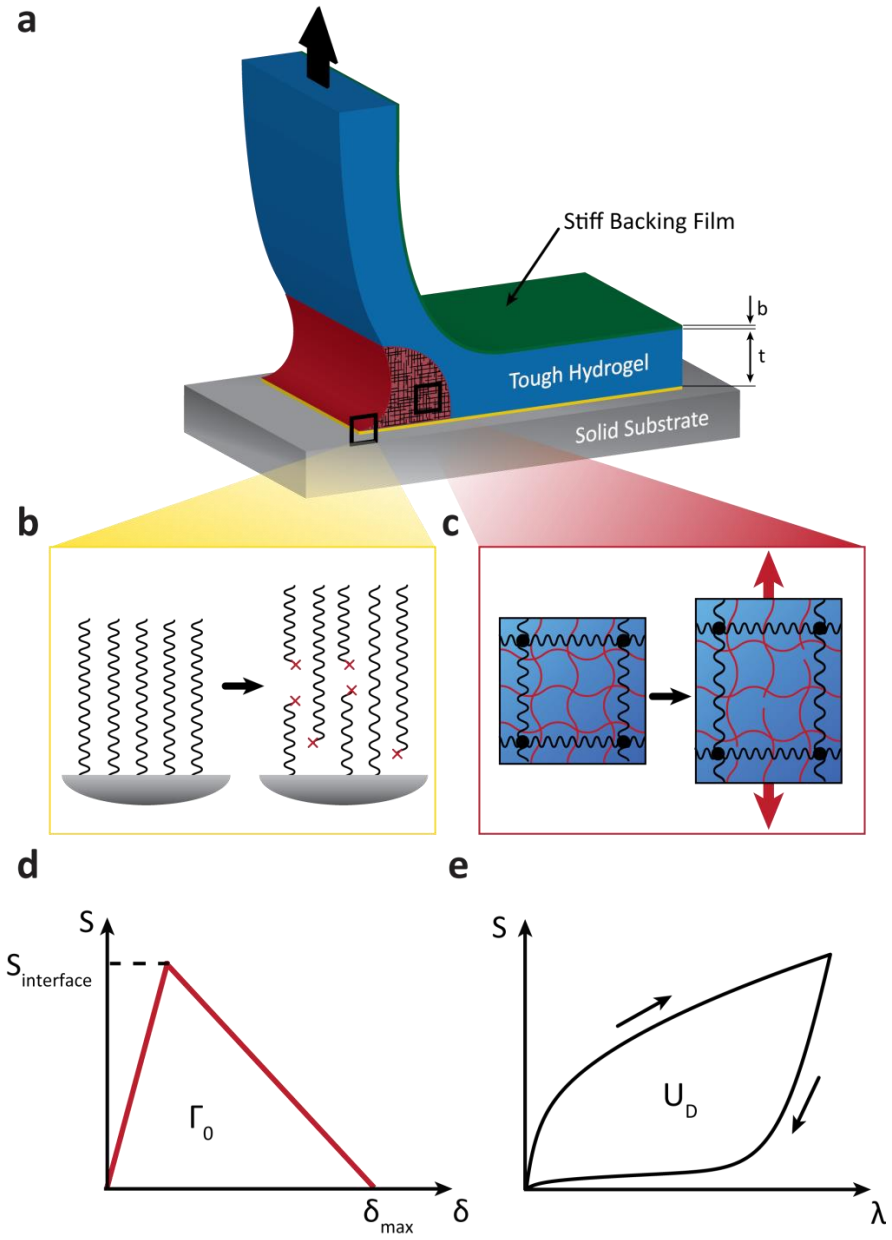

Fig. 2 a-c (Color online) Schematic show of the tough hydrogel during peeling test. The yellow thin layer in plot **a** represent the interface between hydrogel and glass, which is formed by chemical anchoring long chain polymer to the glass surface (plot **b**). The fracture of the polymer chain or its detachment from the glass substrate gives a relatively high intrinsic work of adhesion and high interfacial strength. The dissipation, as shown in plot **c** further contributes to the total interfacial toughness. **d** The interface failure is modeled with a standard cohesive zone model with a triangular traction-separation law. **e** The schematic show of the energy dissipation in the tough hydrogel, which is modeled as the Mullins effect due to the local material damage.

3. Development of the model

Interfacial toughness characterizes the energy required to propagate an interfacial crack by a unit area. The interfacial toughness accounts for the energy for creating new free surfaces, also known as the intrinsic work of adhesion, and the dissipated energy inside the bulk materials (Fig. 2a). For the hydrogel-solid hybrid system, the scission of chemical bonds connecting the hydrogel and the solid substrate gives the intrinsic work of adhesion Γ_0 (Fig. 2b), while the energy dissipation due to deformation of hydrogel near the interface (Fig. 2c) further contributes to the interfacial toughness by the amount of Γ_{D}. Therefore, the total interfacial toughness Γ can be expressed as [27, 30, 31, 39-41, 50]

$$\Gamma = \Gamma_0 + \Gamma_{\mathrm{D}} \ . \tag{1}$$

To describe the intrinsic work of adhesion of the interface, we adopt the cohesive zone model (Fig. 2d). This technique has been employed to simulate the adhesive behaviors of a wide range of materials, including pure elastic [51, 52], viscoelastic [53, 54] and plastic materials [41, 55, 56]. The specific model used in the current study is characterized by a triangular cohesive law with interfacial strength $S_{\mathrm{interface}}$ and maximum separation distance $\delta_{\max}$ (Fig. 2d). The damage of the cohesive interface follows the quadratic nominal stress criterion,

$$\left(\frac{t_n}{S_{\mathrm{interface}}}\right)^2 + \left(\frac{t_s}{S_{\mathrm{interface}}}\right)^2 = 1, \tag{2}$$

where $t_{(\bullet)}$ represents the nominal surface tractions on the crack surface, and the subscripts *n* and *s* indicate normal and tangential directions, respectively. When the surface tractions satisfy the criteria in Eq. (2), the cohesive interface enters into the softening regime, which is described by

the linear damage evolution function depicted in Fig. 2d. The cohesive-zone model prescribes the intrinsic work of adhesion of the hydrogels to be

$$\Gamma_0 = \frac{1}{2} S_{\text{interface}} \delta_{\max} . \tag{3}$$

Since the peeling process is much faster than water diffusion in the hydrogel [27], we model the hydrogel as a hyperealstic material with Mullins effect for energy dissipation. We choose the well-known Ogden-Roxburgh model [57] to characterize the hydrogel in the current study, as this model has been implemented in ABAQUS. The free energy function (i.e., free energy per unit volume of the material at reference state) of a pure hyperelastic material can be expressed as

$$W_{\text{ela}} = W_{\text{dev}} + W_{\text{vol}} = 2\mu \Big/ \left[\alpha^2 \left(\bar{\lambda}_1^{\alpha} + \bar{\lambda}_2^{\alpha} + \bar{\lambda}_3^{\alpha} \right) \right] + \frac{K_0}{2} \left(J - 1 \right)^2 , \tag{4}$$

where W_{ela} is the strain energy density, W_{dev} and W_{vol} denote the deviatoric and volumetric part of the strain energy density, respectively, K_0 and μ denote the initial bulk and shear moduli of the hydrogel, respectively, α the Ogden parameter, $\bar{\lambda}_i = J^{-1/3} \lambda_i$, λ_i the i_{th} principal stretch (i=1,2,3) and J the total volume change. The modified free energy function that incorporates the Mullins effect can be expressed as

$$\bar{W} = \eta W_{\text{dev}} + \phi(\eta) + W_{\text{vol}} , \tag{5a}$$

$$\phi(\eta) = \int_1^{\eta} \left[\left(m + \beta W_{\text{dev}}^{\text{mp}} \right) \text{erf}^{-1} \left(r \left(1 - \eta \right) \right) W_{\text{dev}}^{\text{mp}} \right] \text{d}\eta , \tag{5b}$$

$$\eta = 1 - \frac{1}{r} \text{erf} \left[\left(W_{\text{dev}}^{\text{mp}} - W_{\text{dev}} \right) \Big/ \left(m + \beta W_{\text{dev}}^{\text{mp}} \right) \right] , \tag{5c}$$

where η is a damage variable ($0 < \eta \leq 1$), $W_{\text{dev}}^{\text{mp}}$ denotes the maximum strain energy density in the primary loading, the function $\phi(\eta)$ is referred to as the damage function, erf is the error function, and β is a positive number to avoid overly stiff response at the initiation of unloading

from relatively large stretch levels, and r and m are constants that characterize the damage properties of the material.

A typical stress-strain curve from a loading-unloading cycle is schematically shown in Fig. 2e, where the energy inside the loop will be dissipated and denoted as U_{D}. It has been shown that the energy dissipation U_{D} corresponds to the maximum value of the damage function $\phi(\eta)$ [57, 58]

$$U_{\mathrm{D}} = \phi\left(\eta_{\mathrm{mp}}\right) = \left\{ \mathrm{erf}\left(\frac{W_{\mathrm{dev}}^{\mathrm{mp}}}{m+\beta W_{\mathrm{dev}}^{\mathrm{mp}}} \right) - \frac{m+\beta W_{\mathrm{dev}}^{\mathrm{mp}}}{\sqrt{\pi} W_{\mathrm{dev}}^{\mathrm{mp}}} \left\{ 1 - \exp\left[-\left(\frac{W_{\mathrm{dev}}^{\mathrm{mp}}}{m+\beta W_{\mathrm{dev}}^{\mathrm{mp}}} \right)^2 \right] \right\} \right\} \frac{W_{\mathrm{dev}}^{\mathrm{mp}}}{r}, \quad (6)$$

where $\eta_{\mathrm{mp}} = 1 - \frac{1}{r}\mathrm{erf}\left[W_{\mathrm{dev}}^{\mathrm{mp}} / \left(m + \beta W_{\mathrm{dev}}^{\mathrm{mp}} \right) \right]$ represents the maximum damage of the material. We define the hysteresis ratio of the material under pure-shear tensile deformation as [49]

$$h = U_{\mathrm{D}} / U, \quad (7)$$

where $U = W_{\mathrm{vol}}^{\mathrm{mp}} + W_{\mathrm{dev}}^{\mathrm{mp}}$ and U_{D} are the mechanical work done on and the energy dissipation in a unit volume of the hydrogel under external loading (i.e., pure-shear tensile deformation), respectively. For nearly incompressible materials like hydrogels, we can assume $W_{\mathrm{vol}}^{\mathrm{mp}} \ll W_{\mathrm{dev}}^{\mathrm{mp}}$ so that the hysteresis ratio can be expressed as

$$h = \left\{ \mathrm{erf}\left(\frac{W_{\mathrm{dev}}^{\mathrm{mp}}}{m+\beta W_{\mathrm{dev}}^{\mathrm{mp}}} \right) - \frac{m+\beta W_{\mathrm{dev}}^{\mathrm{mp}}}{\sqrt{\pi} W_{\mathrm{dev}}^{\mathrm{mp}}} \left\{ 1 - \exp\left[-\left(\frac{W_{\mathrm{dev}}^{\mathrm{mp}}}{m+\beta W_{\mathrm{dev}}^{\mathrm{mp}}} \right)^2 \right] \right\} \right\} \frac{1}{r} \quad . \quad (8)$$

Since the hysteresis ratio h can be obtained through cyclic loading of a sample to different maximum stretches, Eq. (8) provides an explicit formula to fit the key parameters in the Ogden-Roxburgh model for Mullins effect, including r, m and β from the experimental measurements. In addition, we use $U_{\mathrm{D}}^{\mathrm{m}}$ and U^{m} to represent the maximum energy dissipation and the maximum

work done in a unit volume of the hydrogel under pure-shear tensile test up to its failure, and define the corresponding maximum hysteresis ratio as

$$h_{\max}=U_{\mathrm{D}}^{\mathrm{m}}/U^{\mathrm{m}}. \tag{9}$$

When $W_{\mathrm{dev}}^{\mathrm{mp}}$ in Eq. (8) is set to be its maximum possible value from pure-shear tensile test (i.e., deformation up to the failure of the material), the hysteresis ratio h in Eq. (8) reaches $h_{\max}$ defined in Eq. (9).

We implement the cohesive-zone and Mullins-effect model into a 2D finite-element model to simulate the 90° peeling test of hydrogels bonded on solid substrates, as shown in the Fig. 2a. The geometry of the hydrogel layer follows the experiments [27], such as thickness equal to 3.2 mm and length 80 mm. The hydrogel layer has a portion initially not bonded to the substrate for gripping during the peeling tests. A stiff backing film (i.e., Young's modulus on the order of GPa, thickness in the range of 10 to 100 μm) is attached on the top of the hydrogel to prevent elongation in the detached part, so that the interfacial toughness can be directly converted from the measured peeling force divided by the sample width [59]. The deformation of the system is assumed to be under plane-strain condition. The material properties associated with the elasticity and dissipation are fitted with previous experimental tests on the hydrogels [27, 48]. The shear modulus μ and the Ogden parameter α are fitted to be 36.57 kPa and 1.473, respectively. The best fitting parameters for the Mullins effect are r = 1.1, m = 4.076 kJ/m^3, and β = 0.2818 [27]. We perform all the numerical simulations with ABAQUS/Explicit [58], where the hydrogel and stiff backing are modeled with CPE4R element, and the cohesive interface is modeled with COH2D element. The Poisson's ratio of the hydrogel is set to be 0.499 to approximate incompressibility. Mass scaling technique is adopted to maintain a quasi-static process during the peeling simulations. To model a quasi-static peeling process with explicit

simulations, we choose the mass scaling parameters that keep the total kinetic energy less than 1% of the total deformation energy. To numerically simulate the 90° peeling test, the left edge of the film is first rotated 90° and then moved vertically at a constant velocity. The reaction force (force per unit length in the 2D simulation) on the left edge of the film is recorded, and the steady-state value gives the interfacial toughness.

Since the 2D finite-element model cannot characterize the fingering instability experimentally observed in peeling tests of hydrogels as shown in Fig. 1c, it is important to verify the predictability of the 2D model before applying it to explain experimental observations. Therefore, we further develop 3D finite-element models for peeling test of hydrogels and compare the stress and energy dissipations from 2D and 3D simulations. The 3D simulation is performed with the C3D8R element with smallest mesh size as 0.1 mm. The cohesive-zone model is not included in this comparison, as it leads to severe numerical instabilities (i.e., element distortions) in 3D simulation. The numerical instabilities may be alleviated by reducing time step in explicit simulation, but this will lead to prohibitively long time simulations and definitely call for more efficient numerical methods for future studies.

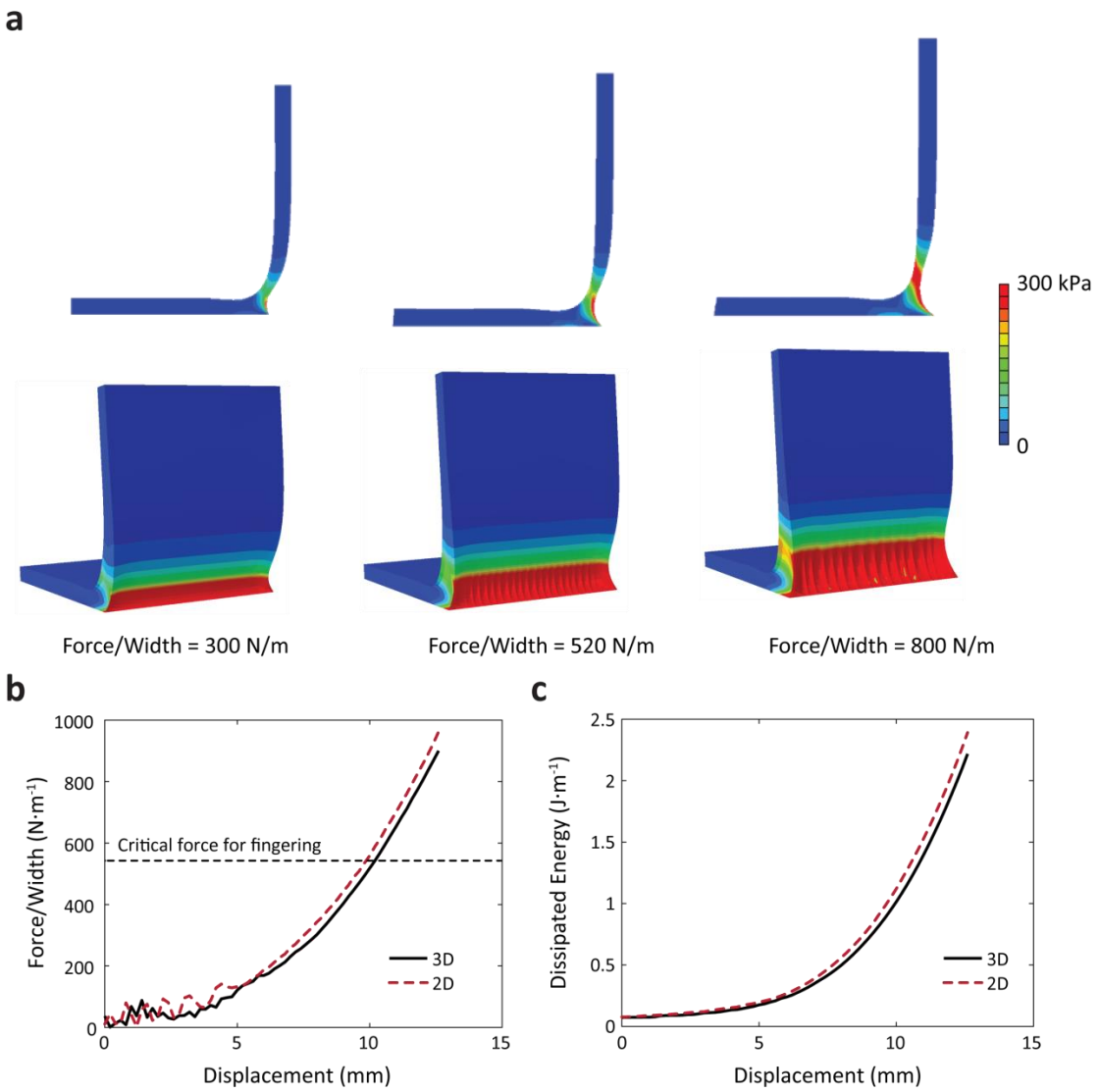

Fig. 3 a (Color online) Von-Mises stress distribution in 2D (top rows) and 3D (bottom rows) simulations for the peeling test at different peeling force showing the initiation and coarsening of the fingering patterns. **b** Simulated curves of the peeling force per width of hydrogel sheet versus displacement for 2D and 3D model. **c** Simulated curves of the total dissipated energy in hydrogel sheet versus displacement for 2D and 3D model.

As shown in Fig. 3a, the 3D finite-element model can successfully capture the initiation and coarsening of fingering patterns with the increase of the peeling force before the propagation of interfacial crack, as observed in the experiments (Fig. 1c**)**. In addition, the critical peeling force for the onset of fingering instability in the simulation is 520 N/m, consistent with the experimental value (300-500 N/m) (shown as supplementary material: Movie S1). Now that we have validated that the 3D model can capture the fingering instability experimentally observed, we will compare its prediction with 2D model's results. Despite missing the fingering patterns, the 2D model indeed predicts very similar reaction force and energy dissipation (both normalized by sample width) as those from the 3D model before crack propagation, as shown in Fig. 3b and 3c, respectively.

4. Comparison of experimental and numerical results of tough and tunable adhesion

It has been known that high intrinsic work of adhesion and high energy dissipation are the key factors for achieving tough hydrogel adhesions [26, 27]. There, however, lacks a systematic study on how the hydrogel geometry and interfacial properties will influence the hydrogel adhesion. In addition, tunable adhesion is also desirable for different applications of hydrogels. For example, while hydrogel glues for biomedical devices may require very tough adhesion, skin adhesives based hydrogels should give moderate adhesion for detachment after usage. To explore the tough and tunable hydrogel adhesions, we conduct a systematic set of experiments and finite-element simulations on the adhesion of polyacrylamide-alginate hydrogels on solid surfaces with different thicknesses of hydrogel layers and interfacial properties.

Thickness effect. The effect of hydrogel-layer thickness on adhesion can be understood as follows. Since the maximum size for the process zone of the interfacial crack cannot exceed the thickness of the hydrogel layer, there is an upper limit for the interfacial toughness of the hydrogel on solid substrates [41],

$$\Gamma_{\max} = \Gamma_0 + U_{\mathrm{D}}^{\mathrm{m}} \vartheta t, \tag{10}$$

where $U_{\mathrm{D}}^{\mathrm{m}}$ denotes the maximum energy dissipation in a unit volume of the hydrogel, t is the thickness of the hydrogel layer, ϑt gives the size of the process zone, and ϑ is a non-dimensional parameter close to unity for thin hydrogel layers. From Eq. (10), we define a critical length scale to determine whether the contribution of mechanical dissipation in the bulk hydrogel to interfacial toughness can be significant

$$l_{\mathrm{c}} = \frac{\Gamma_0}{U_{\mathrm{D}}^{\mathrm{m}}}. \tag{11}$$

If the thickness of the hydrogel is much smaller than the critical length scale, i.e., $t \ll l_{\mathrm{c}}$, the contribution from bulk hydrogel dissipation to interfacial toughness is negligible compared with the intrinsic work of adhesion. Therefore, the interfacial toughness is expected to reach a plateau, Γ_0 as the thickness of the hydrogel layer decreases. On the other hand, when the hydrogel layer is sufficiently thick, the interfacial toughness measured from peeling test is expected to reach another plateau, since only a portion of the hydrogel layer will be significantly deformed to contribute to dissipation during the peeling test.

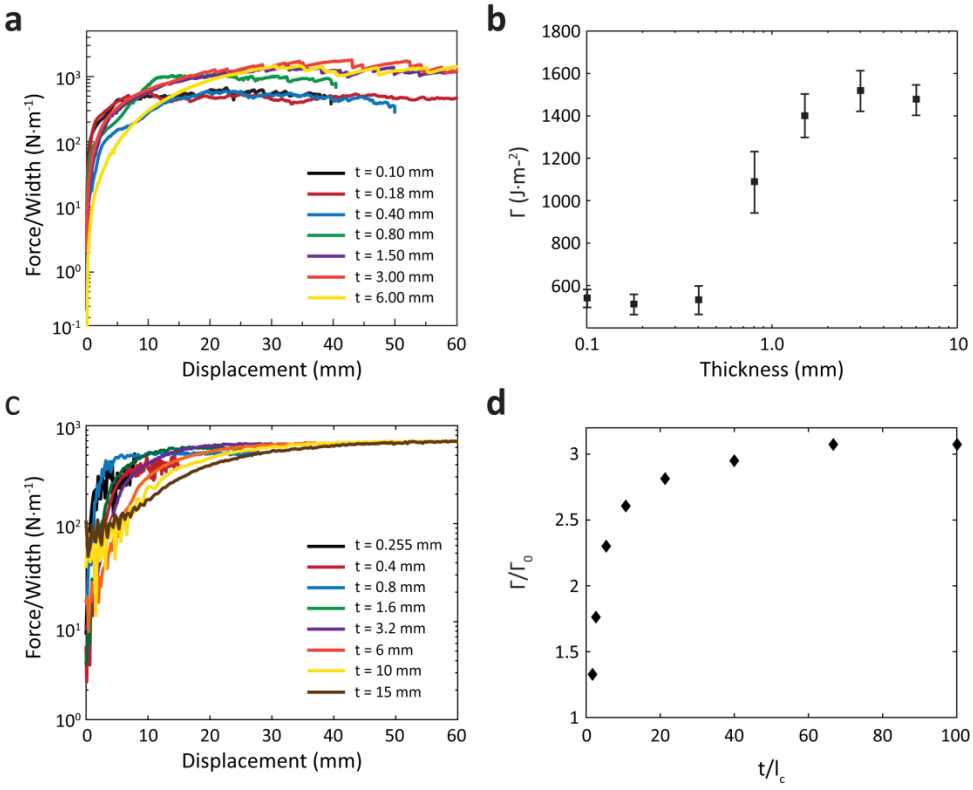

Fig. 4 **a** Experimental curves of the peeling force per width of hydrogel sheet versus displacement for samples with various thickness. **b** The measured interfacial toughness versus the thickness of hydrogel sheet. **c** Simulated curves of the peeling force per width of hydrogel sheet versus displacement for samples with various thickness. **d** The simulated enhancement ratio of the interfacial toughness versus the thickness of hydrogel sheet normalized by the critical length scale, l_c of the hydrogels used here. Values in plot **b** represent the mean and standard deviation (n = 3,4,5).

To quantitatively understand the variation of interfacial toughness with hydrogel thickness, we perform experiments on samples with thickness varying from 0.1 to 6 mm. The curves of peeling force vs. displacement from experiments are given in Fig. 4a and the measured interfacial toughness are summarized in Fig. 4b. Two plateaus of the interfacial toughness can be clearly identified from samples with very thin (e.g., 100 μm) and thick (e.g., 3.2 mm) hydrogel layers, as shown in Fig. 4b. The intrinsic work of adhesion of the hydrogel is thus taken as the experimentally measured interfacial toughness of the lower plateau, which is about 500 J/m^2. (Note this value is higher than reported intrinsic work of adhesion of hydrogels, possibly due to the dissipation induced by complicated deformation in the thin hydrogel layer.) Further taking $U_{\mathrm{D}}^{\mathrm{m}} = 1500\ \mathrm{kJ/m^3}$ [27], the critical length scale l_c can be estimated to be 0.33 mm, consistent with our experimental results. In the corresponding numerical model, we vary the thickness of the hydrogel layer from 0.2 to 15 mm. We further take the interfacial strength $S_{\mathrm{interface}}$ = 300 kPa and maximum separation $\delta_{\max}$ = 1.5 mm. Therefore, the resultant intrinsic work of adhesion is $\Gamma_0 = 225\ \mathrm{J/m^2}$, and the critical length scale $l_{\mathrm{c}} = 0.15\ \mathrm{mm}$ given $U_{\mathrm{D}}^{\mathrm{m}} = 1500\ \mathrm{kJ/m^3}$ [27]. The curves of peeling force vs. displacement from simulations are given in Fig. 4c, and the calculated interfacial toughness is summarized in Fig. 4d. When the hydrogel layer is very thin or very thick, the calculated interfacial toughness from the model also approaches the intrinsic work of adhesion or another higher plateau, respectively, consistent with the theory and experimental results (Fig. 4d). The experiments and simulations further show that the tough hydrogel adhesion can be tuned by controlling the thickness of the hydrogel layer.

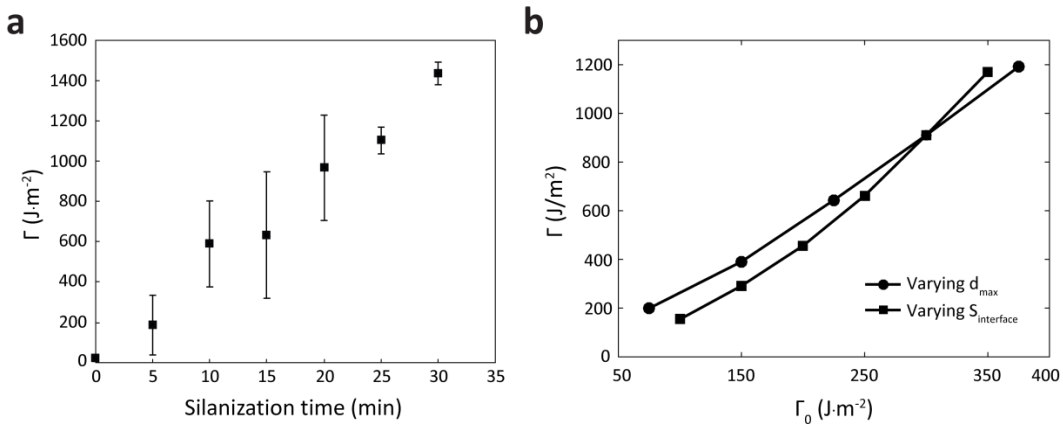

Fig. 5 a Experimentally measured values of the interfacial toughness of the hydrogel versus silanization time of the glass substrate. **b** Interfacial toughness versus the intrinsic work of adhesion obtained from simulation. Values in plot **a** represent the mean and the standard deviation (n = 3,4,5).

Effect of intrinsic work of adhesion. To vary the intrinsic work of adhesion in experiments, we systematically increase the silanization time of the glass substrate from 0 to 30 min. The density of silane molecules on the substrate and thus the density of covalent bonds between the hydrogel and substrate increase with the silanization time [60, 61]. Therefore, the intrinsic work of adhesion and interfacial strength are expected to increase with the silanization time. As shown in Fig. 5a, the measured interfacial toughness indeed increases significantly from 10 to 1000 J/m^2 as the silanization time increases from 0 to 30 min, and they demonstrate an approximately linear relation (Fig. 5a).

In the finite-element model, we correspondingly vary the interfacial strength $S_{\text{interface}}$ and maximum separation $\delta_{\max}$ and thus the intrinsic work of adhesion Γ_0 in two ways: one is varying $\delta_{\max}$ from 0.5 to 2.5 mm while keeping $S_{\text{interface}}$ as 300 kPa, and the other is varying the $S_{\text{interface}}$ from 100 to 350 kPa while keeping $\delta_{\max}$ as 2 mm. The thickness of the hydrogel layer is taken as 3.2 mm in all the simulations, which is thick enough to give the upper plateau of interfacial toughness vs thickness (Fig. 4d). As shown in Fig. 5b, the calculated interfacial toughness Γ increases with the intrinsic work of adhesion Γ_0 approximately linearly for both the cases of varying $S_{\text{interface}}$ and varying $\delta_{\max}$. In addition, the calculated interfacial toughness Γ is indeed multiple times (e.g., ~ 3 times) higher than the corresponding intrinsic work of adhesion Γ_0, due to dissipation in the hydrogel layer under deformation. The experimental and simulation results further confirm the significant tunability of hydrogel adhesions by varying interfacial properties such as interfacial strength and intrinsic work of adhesion.

5. Design principles for tough and tunable adhesion of hydrogels

With the rapid progress of the research on soft materials, it is possible to dramatically tune the bulk material properties of the hydrogels, such as energy dissipation and shear modulus [48, 62, 63]. Taking the polyacrylamide-alginate hydrogel as an example, the shear modulus and energy dissipation can be controlled by changing the concentrations of the ionic and covalent crosslinking densities [48]. Furthermore, the interfacial strength between the hydrogels and solid substrates can be potentially altered by tuning the density of the chemical bonds between hydrogels and solid surfaces. These tunable parameters greatly enlarge the design space for adhesion of hydrogels, and therefore it calls for systematic studies and optimizations of the effects of these parameters. We next perform a parameter study for a modeled hydrogel (i.e., $\alpha = 2$ in Eq. (4)) with different material properties, including the shear modulus (μ) and energy dissipation (m and $h_{\max}$) of the hydrogel and the failure strength ($S_{\text{interface}}$) of the cohesive interface. From the dimensionless analysis, we can have the following functional form for the interfacial toughness enhancement

$$\frac{\Gamma}{\Gamma_0} = G\left(\frac{S_{\text{interface}}}{\mu}, \frac{m}{\mu}, h_{\max}\right), \tag{12}$$

where Γ refers to the interfacial toughness for a sufficiently thick hydrogel layer (i.e., toughness reaches the higher plateau) and G is a dimensionless function for the interfacial toughness enhancement.

A series of simulations have been conducted to explore the influence of each dimensionless variable ($S_{\text{interface}}/\mu, m/\mu$ and $h_{\max}$) on the final interfacial toughness by varying one parameter at a time. For the simulations in this section, we set the film thickness t to be 3.2 mm, the film shear modulus to be 1 kPa, the intrinsic work of adhesion Γ_0 to be 4 J/m^2, and the

numerical parameter β in Eq. (5) to be 0.1. We vary the damage parameter r in Eq. (5) to tune the maximum hysteresis ratio h_{max} and calculate the associated interfacial toughness with finite-element simulations. In these calculation, we further change m and $S_{interface}$ to investigate their influences on the relationship between interfacial toughness and h_{max}.

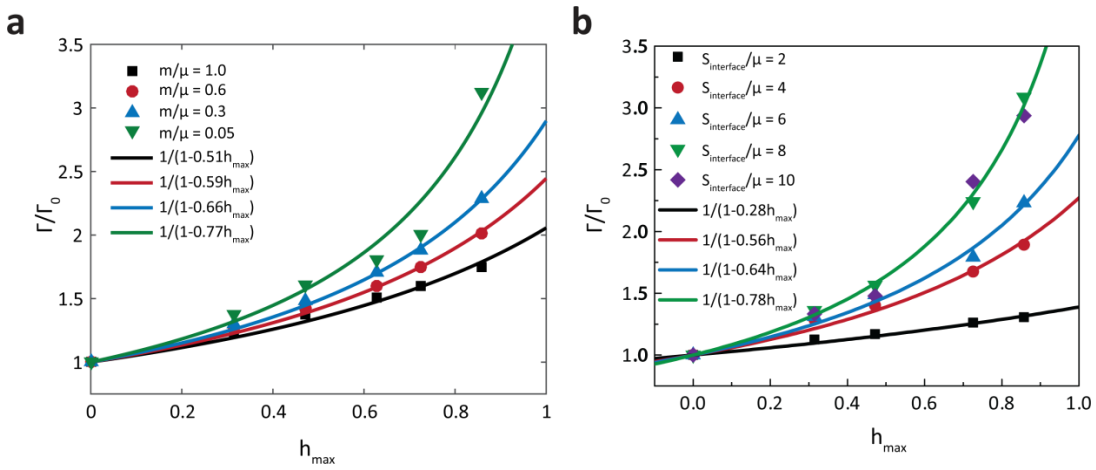

Fig. 6 a The effect of energy threshold for activating energy dissipation *m* of the bulk hydrogel sheet and interfacial strength on the interfacial toughness. The enhancement ratio of the interfacial toughness versus the maximum energy dissipation ratio h_{max} for different *m*. **b** The enhancement ratio of the interfacial toughness versus the maximum energy dissipation ratio h_{max} for various interfacial strengths.

We first discuss the effects of m and h_{max} on the calculated interfacial toughness. In this set of simulations, we set the interfacial strength as $S_{interface}/\mu = 8$ and δ_{max} = 1 mm. Figure 6a shows the corresponding interfacial toughness as a function of h_{max} for different m. It can be seen that the interfacial toughness monotonically increases with h_{max} and decreases with m. This trend can be understood as follow. For hydrogels with the same m, a larger value of h_{max} gives higher capability of energy dissipation and therefore higher enhancement of the interfacial toughness. On the other hand, for hydrogels with the same h_{max}, a smaller value of m (normalized by the shear modulus μ) gives a faster transition from the low energy-dissipation state to the high energy-dissipation state of the hydrogel [49], which leads to higher enhancement of the interfacial toughness.

We then investigate the influence of the interfacial strength $S_{interface}$ (normalized by the shear modulus μ) and h_{max} on the interfacial toughness. In this set of simulations, we adjust the maximum separation δ_{max} accordingly to maintain the intrinsic work of adhesion Γ_0 constant. The m parameter is also taken to be zero in this set of simulations. The calculated interfacial toughness for different values of $S_{interface}$ and h_{max} are presented in Fig. 6b. For hydrogels with the same h_{max}, the interfacial toughness increases with $S_{interface}$. This is consistent with the experimental observation that a higher density of covalent crosslinkings between hydrogel polymers and substrate gives higher $S_{interface}$ and tougher interface.

Interestingly, the relation between the interfacial toughness enhancement and h_{max} for different values of m and $S_{interface}$ can be well described by the following equation with one fitting coefficient χ

$$\frac{\Gamma}{\Gamma_0} = \frac{1}{1-\chi h_{max}} \ , \tag{13}$$

which follows a similar form for the fracture toughness enhancement of hydrogels due to the Mullins effect [49]. From the above sets of simulations (Fig. 6), we further show that the fitting coefficient χ defined in Eq. (13) is a monotonic increasing function of $S_{\text{interface}}/\mu$ and monotonic decreasing function of m/μ.

6. Conclusions and discussions

In this paper, we combine experiments and numerical simulations to explain the mechanisms for tough and tunable adhesion of hydrogels on solid substrates. The tough adhesion relies on chemically anchoring stretchy polymer networks in tough hydrogels on solid substrates, which gives high intrinsic work of adhesion to trigger significant energy dissipation of the bulk hydrogel during detachment [26, 27]. We show that the hydrogel-solid interfacial toughness linearly scales with its intrinsic work of adhesion, and the contribution form energy dissipation of the bulk hydrogel to the interfacial toughness can be much higher than the intrinsic work of adhesion. In addition, our experiments and simulations capture the dependence of interfacial toughness on the thickness of hydrogel layer. A critical length scale has been defined to estimate whether the contribution from mechanical dissipation in the bulk hydrogel to interfacial toughness is significant. When the thickness of the hydrogel layer is much larger or smaller than the critical length, the interfacial toughness reaches two plateaus, respectively. When the hydrogel thickness is comparable with the critical length, the interfacial toughness increases monotonically with the hydrogel thickness, which prescribes the size of process zone. Our experiments and simulations also show that the interfacial toughness can be significantly tuned by varying the density of chemical anchorage of hydrogel polymers on solid surfaces. We further explore the principles to design tough and adhesive soft materials by systematically

varying their bulk and interfacial properties. For a material with given shear modulus and intrinsic work of adhesion, it is found that high interfacial strength and capacity of energy dissipation (i.e., large values of $h_{\max}$ and $S_{\text{interface}}/\mu$ and small value of m) are key to the significant enhancement of interfacial toughness.

Although the current model can reasonably predict the enhancement of interfacial toughness compared with experiments, a number of factors, including fingering instabilities, cavitation and viscoelasticity, are not included yet and deserve future studies. The current model utilizes experimentally measured bulk mechanical properties of the tough hydrogels but requires the fitting of interfacial strength $S_{\text{interface}}$ and maximum separation distance $\delta_{\max}$ of the cohesive zone to compare with experiments. It is highly desirable to develop a multiscale model to incorporate the values of $S_{\text{interface}}$ and $\delta_{\max}$ calculated from molecular-scale models into the current continuum model.

Beyond the intrinsic material properties, the geometry of the adhered structures will also influence the overall adhesion, a strategy widely adopted in nature, such as the adhesion of gecko [64] and mussel [3]. The hierarchical structure in gecko's feet is utilized to achieve a strong and reversible adhesion from weak van der Waals interactions [65]. Although mussel's superior under water adhesion is usually attributed to chemicals like DOPA [17, 18], it is recently shown that mussel also optimizes the plaque shape and the mechanical properties of thread to further achieve significant enhancements of the interfacial toughness compared to the plaque material itself [4]. It would be interesting to explore other strategies for the design of adhesive, soft tough materials from the structure optimization inspired by nature, such as Gecko and Mussel adhesion.

Acknowledgments

This work is supported by the Office Naval Research (No. N00014-14-1-0528), Draper Laboratory, MIT Institute for Soldier Nanotechnologies and the National Science Foundation (No. CMMI-1253495). Hyunwoo Yuk acknowledges the financial support from Samsung Scholarship. Xuanhe Zhao acknowledges the supports from the National Institutes Health (No. UH3TR000505). The authors are also grateful for the support from MIT research computing resources and the Extreme Science and Engineering Discovery Environmen (XSEDE) (No. TG-MSS160007).

Reference

1. Bobyn, J., Wilson, G., MacGregor, D., et al.: Effect of pore size on the peel strength of attachment of fibrous tissue to porous-surfaced implants. J. Biomed. Mater. Res. **16**, 571-584 (1982).
2. Moretti, M., Wendt, D., Schaefer, D., et al.: Structural characterization and reliable biomechanical assessment of integrative cartilage repair. J. Biomech. **38**, 1846-1854 (2005).
3. Waite, J.H.: Nature's underwater adhesive specialist. Int. J. Adhes. Adhes. **7**, 9-14 (1987).
4. Desmond, K.W., Zacchia, N.A., Waite, J.H., et al.: Dynamics of mussel plaque detachment. Soft matter. **11**, 6832-6839 (2015).
5. Qin, Z.,Buehler, M.J.: Impact tolerance in mussel thread networks by heterogeneous material distribution. Nat. Commun. **4**, (2013).
6. Peppas, N.A., Hilt, J.Z., Khademhosseini, A., et al.: Hydrogels in biology and medicine: from molecular principles to bionanotechnology. Adv. Mater. **18**, 1345 (2006).
7. Lee, K.Y.,Mooney, D.J.: Hydrogels for tissue engineering. Chem. Rev. **101**, 1869-1880 (2001).
8. Keplinger, C., Sun, J.-Y., Foo, C.C., et al.: Stretchable, transparent, ionic conductors. Science. **341**, 984-987 (2013).
9. Lin, S., Yuk, H., Zhang, T., et al.: Stretchable hydrogel electronics and devices. Adv. Mater. **28**, 4497–4505 (2016).
10. Dong, L., Agarwal, A.K., Beebe, D.J., et al.: Adaptive liquid microlenses activated by stimuli-responsive hydrogels. Nature. **442**, 551-554 (2006).
11. Beebe, D.J., Moore, J.S., Bauer, J.M., et al.: Functional hydrogel structures for autonomous flow control inside microfluidic channels. Nature. **404**, 588-590 (2000).
12. Yu, C., Duan, Z., Yuan, P., et al.: Electronically Programmable, Reversible Shape Change in Two- and Three-Dimensional Hydrogel Structures. Adv. Mater. **25**, 1541-1546 (2013).
13. Sudre, G., Olanier, L., Tran, Y., et al.: Reversible adhesion between a hydrogel and a polymer brush. Soft Matter. **8**, 8184-8193 (2012).
14. Peak, C.W., Wilker, J.J., Schmidt, G.: A review on tough and sticky hydrogels. Colloid Polym. Sci. **291**, 2031-2047 (2013).
15. Wu, C.J., Wilker, J.J., Schmidt, G.: Robust and Adhesive Hydrogels from Cross-Linked Poly (ethylene glycol) and Silicate for Biomedical Use. Macromol. Biosci. **13**, 59-66 (2013).
16. Rose, S., Prevoteau, A., Elzière, P., et al.: Nanoparticle solutions as adhesives for gels and biological tissues. Nature. **505**, 382-385 (2014).
17. Waite, J.H.,Tanzer, M.L.: Polyphenolic substance of Mytilus edulis: novel adhesive containing L-dopa and hydroxyproline. Science. **212**, 1038-1040 (1981).
18. Lee, H., Scherer, N.F., Messersmith, P.B.: Single-molecule mechanics of mussel adhesion. Proc. Natl. Acad. Sci. U.S.A. **103**, 12999-13003 (2006).
19. Qin, Z.,Buehler, M.J.: Molecular mechanics of mussel adhesion proteins. J. Mech. Phys. Solids. **62**, 19-30 (2014).
20. Lin, Q., Gourdon, D., Sun, C., et al.: Adhesion mechanisms of the mussel foot proteins mfp-1 and mfp-3. Proc. Natl. Acad. Sci. U.S.A. **104**, 3782-3786 (2007).

21. Brubaker, C.E.,Messersmith, P.B.: Enzymatically degradable mussel-inspired adhesive hydrogel. Biomacromolecules. **12**, 4326-4334 (2011).
22. Guvendiren, M., Messersmith, P.B., Shull, K.R.: Self-assembly and adhesion of DOPA-modified methacrylic triblock hydrogels. Biomacromolecules. **9**, 122-128 (2007).
23. Lee, B.P., Dalsin, J.L., Messersmith, P.B.: Synthesis and gelation of DOPA-modified poly (ethylene glycol) hydrogels. Biomacromolecules. **3**, 1038-1047 (2002).
24. Kim, B.J., Oh, D.X., Kim, S., et al.: Mussel-Mimetic Protein-Based Adhesive Hydrogel. Biomacromolecules. **15**, 1579-1585 (2014).
25. Kurokawa, T., Furukawa, H., Wang, W., et al.: Formation of a strong hydrogel–porous solid interface via the double-network principle. Acta Biomater. **6**, 1353-1359 (2010).
26. Yuk, H., Zhang, T., Parada, G.A., et al.: Skin-inspired hydrogel-elastomer hybrids with robust interfaces and functional microstructures. Nat. Commun. **7**, (2016).
27. Yuk, H., Zhang, T., Lin, S., et al.: Tough bonding of hydrogels to diverse non-porous surfaces. Nat. Mater. **15**, 190-196 (2016).
28. Gent, A.,Lai, S.M.: Interfacial bonding, energy dissipation, and adhesion. J. Polym. Sci. Part B. **32**, 1543-1555 (1994).
29. Creton, C., Kramer, E.J., Brown, H.R., et al.: Adhesion and fracture of interfaces between immiscible polymers: from the molecular to the continuum scal, in Molecular Simulation Fracture Gel Theory. Springer, Berlin Heidelberg, 53-136 (2001).
30. Shull, K.R.: Contact mechanics and the adhesion of soft solids. Mater. Sci. Eng. R-Rep. **36**, 1-45 (2002).
31. Creton, C.,Ciccotti, M.: Fracture and adhesion of soft materials: a review. Rep. Prog. Phys. **79**, 046601 (2016).
32. Ahagon, A.,Gent, A.: Effect of interfacial bonding on the strength of adhesion. J. Polym. Sci. Polym. Phys. Ed. **13**, 1285-1300 (1975).
33. Gent, A.: Adhesion and strength of viscoelastic solids. Is there a relationship between adhesion and bulk properties? Langmuir. **12**, 4492-4496 (1996).
34. Derail, C., Allal, A., Marin, G., et al.: Relationship between viscoelastic and peeling properties of model adhesives. Part 1. Cohesive fracture. J. Adhesion. **61**, 123-157 (1997).
35. Derail, C., Allal, A., Marin, G., et al.: Relationship between viscoelastic and peeling properties of model adhesives. Part 2. The interfacial fracture domains. J. Adhesion. **68**, 203-228 (1998).
36. Xu, D.B., Hui, C.Y., Kramer, E.J.: Interface fracture and viscoelastic deformation in finite size specimens. J. Appl. Phys. **72**, 3305-3316 (1992).
37. Creton, C.: Pressure-sensitive adhesives: an introductory course. MRS bulletin. **28**, 434-439 (2003).
38. Villey, R., Creton, C., Cortet, P.-P., et al.: Rate-dependent elastic hysteresis during the peeling of pressure sensitive adhesives. Soft matter. **11**, 3480-3491 (2015).
39. Kim, K.S.,Aravas, N.: Elastoplastic analysis of the peel test. Int. J. Solids. Struct. **24**, 417-435 (1988).
40. Kim, K.-S.,Kim, J.: Elasto-plastic analysis of the peel test for thin film adhesion. J. Eng. Mater. Tech. **110**, 266-273 (1988).
41. Wei, Y.,Hutchinson, J.W.: Interface strength, work of adhesion and plasticity in the peel test. Int. J. Fract. **93**, 315-333 (1998).

42. Persson, B., Albohr, O., Tartaglino, U., et al.: On the nature of surface roughness with application to contact mechanics, sealing, rubber friction and adhesion. J. Phys. Condens. Matter. **17**, R1 (2005).
43. Hoefnagels, J., Neggers, J., Timmermans, P., et al.: Copper–rubber interface delamination in stretchable electronics. Scr. Mater. **63**, 875-878 (2010).
44. Vossen, B.G., Schreurs, P.J., van der Sluis, O., et al.: Multi-scale modeling of delamination through fibrillation. J. Mech. Phys. Solids. **66**, 117-132 (2014).
45. Neggers, J., Hoefnagels, J., van der Sluis, O., et al.: Multi-scale experimental analysis of rate dependent metal–elastomer interface mechanics. J. Mech. Phys. Solids. **80**, 26-36 (2015).
46. Vossen, B., van der Sluis, O., Schreurs, P., et al.: High toughness fibrillating metal-elastomer interfaces: On the role of discrete fibrils within the fracture process zone. Eng. Fract. Mech. (2016).
47. Gong, J.P., Katsuyama, Y., Kurokawa, T., et al.: Double-network hydrogels with extremely high mechanical strength. Adv. Mater. **15**, 1155-1158 (2003).
48. Sun, J.-Y., Zhao, X., Illeperuma, W.R., et al.: Highly stretchable and tough hydrogels. Nature, **489**, 133-136 (2012).
49. Zhang, T., Lin, S., Yuk, H., et al.: Predicting fracture energies and crack-tip fields of soft tough materials. Extreme Mech. Lett. **4**, 1-8 (2015).
50. Maugis, D.,Barquins, M.: Fracture mechanics and the adherence of viscoelastic bodies. J. Phys. D: Appl. Phys., **11**, 1989-2023 (1978).
51. Rahul-Kumar, P., Jagota, A., Bennison, S., et al.: Polymer interfacial fracture simulations using cohesive elements. Acta Mater. **47**, 4161-4169 (1999).
52. Mohammed, I.,Liechti, K.M.: Cohesive zone modeling of crack nucleation at bimaterial corners. J. Mech. Phys. Solids. **48**, 735-764 (2000).
53. Rahulkumar, P., Jagota, A., Bennison, S., et al.: Cohesive element modeling of viscoelastic fracture: application to peel testing of polymers. Int. J. Solids. Struct. **37**, 1873-1897 (2000).
54. Allen, D.H., Searcy, C.R.: A micromechanical model for a viscoelastic cohesive zone. International Journal of Fracture, **107**, 159-176 (2001).
55. Yang, Q., Thouless, M., Ward, S.: Numerical simulations of adhesively-bonded beams failing with extensive plastic deformation. J. Mech. Phys. Solids. **47**, 1337-1353 (1999).
56. Su, C., Wei, Y., Anand, L.: An elastic–plastic interface constitutive model: application to adhesive joints. Int. J. Plast. **20**, 2063-2081 (2004).
57. Ogden, R.,Roxburgh, D. A pseudo–elastic model for the Mullins effect in filled rubber. Proc. R. Soc. A. 455, 2861-2877 (1999).
58. Systèmes, D.: Abaqus analysis user's manual. Simulia Corp. Providence, RI, USA, (2007).
59. Kendall, K.: Thin-film peeling-the elastic term. J. Phys. D: Appl. Phys. **8**, 1449 (1975).
60. Kanan, S.M., Tze, W.T., Tripp, C.P.: Method to double the surface concentration and control the orientation of adsorbed (3-aminopropyl) dimethylethoxysilane on silica powders and glass slides. Langmuir. **18**, 6623-6627 (2002).
61. Moon, J.H., Shin, J.W., Kim, S.Y., et al.: Formation of uniform aminosilane thin layers: an imine formation to measure relative surface density of the amine group. Langmuir. **12**, 4621-4624 (1996).

62. Sun, T.L., Kurokawa, T., Kuroda, S., et al.: Physical hydrogels composed of polyampholytes demonstrate high toughness and viscoelasticity. Nat. Mater. **12**, 932-937 (2013).
63. Ducrot, E., Chen, Y., Bulters, M., et al.: Toughening elastomers with sacrificial bonds and watching them break. Science. **344**, 186-189 (2014).
64. Autumn, K., Liang, Y.A., Hsieh, S.T., et al.: Adhesive force of a single gecko foot-hair. Nature. **405**, 681-685 (2000).
65. Yao, H.,Gao, H.: Mechanics of robust and releasable adhesion in biology: Bottom–up designed hierarchical structures of gecko. J. Mech. Phys. Solids. **54**, 1120-1146 (2006).